# Triad-LMF: A Hierarchical Low-Rank Multimodal Fusion Framework for Robust Cancer Subtype Classification Using Multi-Omics Data

**Xingyue Tan [1†], Xiran Chen [1,2†], Zhuangzhuang Ren [1,*], Renjie Tian [3], Miaoyuan Jiang [1], Dongqiu Yang [1], Xianghui Guo [1]**

[1] *School of Mathematics and Statistics, Chongqing Jiaotong University, Chongqing 400074*
[2] *Research Center on Neural Networks and Machine Learning, Chongqing Jiaotong University, Chongqing, 400074, China*
[3] *Institute of Computer Vision and Traffic Image Understanding, School of Information Science and Engineering, Chongqing Jiaotong University, Chongqing 400074, China*
[†] *These authors have contributed equally to this work and share the first authorship*

Correspondence*:
Zhuangzhuang Ren
StrongRen.horizon@mails.cqjtu.edu.cn

## ABSTRACT

Cancer heterogeneity is recognized as a major barrier to precise molecular subtype classification. Conventional approaches inadequately leverage the complementary nature of multimodal data, resulting in overfitting when handling high-dimensional omics data and constraining the comprehensive characterization of cancer subtype heterogeneity. To address this, Triad-LMF, a novel multi-omics integration framework, is introduced, leveraging a low-rank multimodal fusion mechanism to improve the Accuracy of cancer subtype classification. Triad-LMF consolidates multi-omics datasets, mitigating feature dimension disparities through optimized preprocessing. To enable efficient multimodal information integration, Triad-LMF implements a two-stage hierarchical fusion strategy, where in Local Pairwise Fusion and Global Triadic Fusion are combined via the Two-Feature and Three-way LMF modules, facilitating a progressive transition from local modality interactions to global feature integration. Experimental results demonstrate that Triad-LMF outperforms traditional machine learning methods and previous published methods in classification performance. UMAP verifies that Global Triadic Fusion significantly enhances the ability to discriminate against subtypes in implicit space representation. We further illustrate the effectiveness of Triad-LMF in making full use of multimodal interactive information. Additionally, SHAP feature importance analysis was adopted for extracting the important features. Moreover, across independent datasets, Triad-LMF demonstrates superior generalization capabilities. Triad-LMF offers an efficient and robust framework for multi-omics-driven cancer subtype classification.

**Keywords: Cancer subtyping, Deep learning, supervised learning, low-rank multi-modal fusion, hierarchy network**

## 1 INTRODUCTION

The high heterogeneity of cancer makes its molecular subtype classification a key cornerstone of precision medicine (Chen et al. (2020)). In recent years, the rapid development of multi-omics data has provided unprecedented opportunities to uncover molecular mechanisms of cancer, identify subtype-specific biomarkers, and guide personalized therapy (Gao et al. (2022)). By integrating multimodal data such as gene expression, epigenetics, proteomics, and pathology images, researchers can more comprehensively depict the biological characteristics of cancer. However, the high dimensionality of multi-omics data, the complex interactions between modalities,and data heterogeneity pose severe challenges to traditional computational methods. Therefore, developing novel integration frameworks that efficiently fuse these data is urgently needed to advance cancer subtype classification and precision medicine.

Supervised learning methods hold a significant position in cancer subtype classification models due to their ability to substantially improve classification Accuracy by leveraging labeled data. These methods mine subtype-specific patterns by integrating gene expression, mutation data, and other omics features, demonstrating excellent performance across cancer types such as breast cancer and colorectal cancer (Yang et al. (2019)); Singh et al. (2022);Li et al. (2022)). By optimizing model architectures and feature selection strategies, they enhance robustness against sparse or high-dimensional data, providing strong support for precise diagnosis and treatment. However, the limitations of existing methods cannot be overlooked: many adopt a one-time fusion strategy, making it challenging to capture dynamic interactions among modalities (Li et al. (2022); Wang et al. (2021)); handling high-dimensional data often leads to overfitting, especially pronounced in deep learning models(Kuang et al. (2023); Yin et al. (2022)). These shortcomings constrain the further application of multi-omics data in precision medicine.

Based on the challenges above, we believe the fundamental issue of current models lies in the lack of hierarchical fusion mechanisms and explicit modeling of modality interactions, which limits the depth of biological pattern mining, while overfitting issues undermine model generalization. Therefore, this study proposes the Triad-LMF model, which introduces the following innovative designs to achieve breakthroughs in multi-omics data integration and subtype classification:

- Triad-LMF first explicitly models modality-specific interactions through the Two-Feature LMF module, followed by high-level integration via the Three-way LMF module. This hierarchical design overcomes the limitations of traditional one-step fusion. Compared with existing methods, this strategy captures dynamic interactions between modalities through stepwise fusion, significantly improving classification performance.
- Low-rank decomposition techniques are introduced at all fusion stages. By enforcing low-rank constraints, the nonlinear modeling capability is enhanced while the number of parameters is significantly reduced, effectively alleviating overfitting issues caused by high-dimensional data and providing a feasible solution for large-scale multi-omics data analysis.
- Triad-LMF prioritizes learning joint representations of specific modality pairs through the Two-Feature LMF module, generating interpretable interaction features that improve model robustness. It also offers biological insights into the contribution of modality pairs to subtype classification, deepening the exploration compared to existing methods and providing new perspectives for identifying subtype-specific biomarkers.

## 2 RELATED WORK

### 2.1 Unsupervised Learning

Unsupervised learning methods mine potential subtypes through clustering or dimensionality reduction. For example, Guo et al. (2020)proposed a kernel fusion approach that integrates gene expression, miRNA expression, and isoform data to construct similarity kernel matrices, thereby efficiently clustering breast cancer and lung cancer subtypes. This method uses kernel functions to capture nonlinear relationships between modalities and demonstrates high subtype discrimination capability on the TCGA dataset. However, its simple fusion strategy makes it difficult to model hierarchical interactions between modalities, limiting the analysis of complex biological patterns. Liu et al. (2021) developed a multiview spectral clustering method (MRF-MSC) that fuses multi-omics data through multi-smooth representations and combines spectral clustering to uncover subtype structures, showing excellent performance across multiple cancer types in the TCGA dataset.Liu et al. (2024) discovered subtypes through dual self-supervised learning for clustering cancer subtypes, significantly improving the model's generalization capability. Nevertheless, the fusion process of this method overlooks dynamic interactions between modalities, restricting its application in highly heterogeneous data.

### 2.2 Supervised Learning

To achieve higher classification Accuracy, supervised learning methods leverage labeled data to improve cancer subtype classification performance significantly. BCDForest by Yang et al. (2019) optimizes subtype classification of small-scale gene expression data through multi-granularity scanning and enhances model robustness to sparse data via random forests and multi-scale feature selection strategies; however, its performance is limited when generalized to large-scale multi-omics datasets. DeepCSD by Singh et al. (2022) employs a minimalist feedforward neural network combined with gene expression and mutation data to identify colorectal cancer subtypes efficiently. It benefits from low computational complexity but has limited capacity to capture complex biological features. Li et al. (Li et al. (2022); Li et al. (2024); Lin et al. (2020)) utilize graph convolutional networks (GCNs) to integrate multi-omics data by constructing inter-modality relation graphs, demonstrating excellent performance in breast cancer and pan-cancer classification. These works exploit graph neural networks to mine topological relationships between modalities but suffer from high model complexity, easily leading to overfitting. (Wang et al. (2021); Wang et al. (2024); Wang et al. (2023)) optimize classification and biomarker identification through GCNs and graph attention networks (GATs), combining attention mechanisms to prioritize key features, further enhancing cancer subtype classification Accuracy and interpretability. Sun et al. (2022) perform multi-class classification using co-expression modules, mining gene co-expression patterns to strengthen the model's biological relevance, but remains insufficient in modality fusion.Yin et al. (2022) propose a robust GCN framework that stabilizes high-dimensional data through regularization optimization, achieving excellent performance in pan-cancer subtype classification. (Zhang et al. (2022)) model molecular mechanisms via gene interaction networks, significantly improving subtype classification Accuracy. Although these supervised methods excel in Accuracy, their one-time fusion strategies struggle to model dynamic interactions between modalities, and handling high-dimensional data often leads to overfitting issues.

### 2.3 Semi-Supervised Learning

In scenarios with limited annotated data, semi-supervised learning offers a compromise solution. DeepType by Chen et al. (2020) integrates supervised classification and unsupervised clustering, effectively

leveraging the limited labeled information in the TCGA dataset through joint optimization of labeled and unlabeled data, demonstrating excellent breast cancer subtype classification performance. Gao et al. (2022) mined nonlinear features using a semi-supervised model that combines autoencoders and regularization techniques, enhancing the model's generalization ability on small sample datasets. Ramirez et al. (2022) utilized multi-omics autoencoders to predict breast cancer subtypes, uncovering latent features through nonlinear dimensionality reduction and improving model robustness.Zhao et al. (2022) optimized classification performance by incorporating consistency regularization, enhancing classification Accuracy by constraining model consistency on unlabeled data. Wu et al. (2022) modeled gene mutation data via mutation networks combined with graph neural networks to optimize classification, showing potential in pan-cancer subtype classification. However, these fusion methods still exhibit insufficient modeling of modality interactions, making it difficult to capture the complex relationships in multi-omics data comprehensively.

## 3 METHODS

This paper proposes a deep learning framework called Triad-LMF based on Low-rank Multimodal Fusion (LMF). Inspired by (Sahay et al. (2020)), this method efficiently fuses heterogeneous omics data through modality-specific low-rank factors, overcoming the limitations of traditional tensor fusion methods and generating a unified low-dimensional representation for downstream cancer subtype identification. Figure 1 shows the framework of Triad-LMF. We describe each block in more detail in the following.

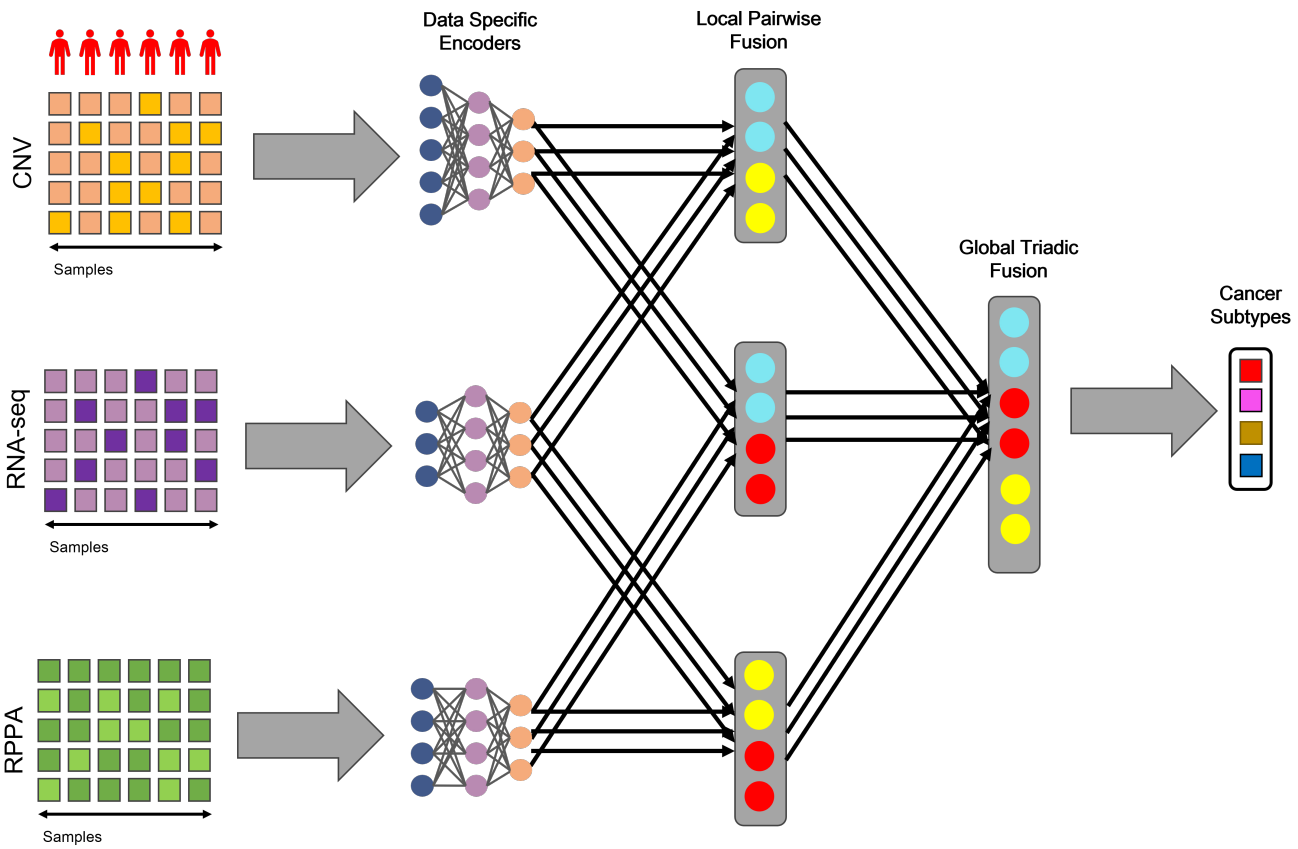


**Figure 1.** The framework of Triad-LMF

## 3.1 Modility-Specific Feature Extractor Encoder

Multi-omics data typically exhibit high dimensionality, heterogeneity, and noise interference, which pose significant challenges for feature extraction. For example, the RNA-seq data in the BRCA dataset contains 16,383 features, where RPPA includes only 223 features. This discrepancy in dimensionality and data noise may obscure underlying biological patterns. To address this, we designed a Modality-Specific Embedding Subnetwork.

Given a set of cancer multi-omics data $X = \{X_1, X_2, \ldots, X_N\}$,$X_i \in R^{B\times d_i}, i = 1, 2, \ldots, N$, where $N$ is the number of datasets, $X_i$ is the input data of modality $i$, with $d_i$ as the input dimension of modality. To extract the hidden representations $\hat{X}_i \in R^{B\times \hat{d}_i}$ of nonlinear features for each modality. Each omics is assigned with Modality-specific Encoder $\hat{X}_i = f_i(X_i)$

## 3.2 Low-rank Multimodal Fusion

Integrating representations from multiple modalities to capture cross-modal interaction information in multi-omics data analysis is crucial for achieving precise cancer subtype classification. However, traditional multimodal fusion methods often result in exponential growth in computational complexity when dealing with high-dimensional data, which is impractical for real-world applications. We designed Low-rank Multimodal Fusion modules that significantly reduce computational complexity by introducing modality-specific low-rank factors to address this issue. We propose two variants for this purpose:

- Local Pairwise Fusion for pairwise modality fusion
- Global Triadic Fusion is used to integrate all modalities.

### 3.2.1 Local Pairwise Fusion

Given the representation of two modalities $X_1 \in R^{B\times h_1}$ and $X_2 \in R^{B\times h_2}$, respectively, the fused output representation generated by the two feature LMF is $Z \in R^{B\times r}$, where $r$ is the rank parameter. To introduce a bias term and enhance the flexibility of the representation, we first extend the hidden representations:

$$X_1^{'} = [1, X_1] \in R^{B\times(h_1+1)} \tag{1}$$

$$X_2^{'} = [1, X_2] \in R^{B\times(h_2+1)} \tag{2}$$

where $1$ is an all-one vector.

The fusion process uses modality specific low-rank factors $F_1 \in R^{r\times(h_1+1)\times d_y}$ and $F_2 \in R^{r\times(h_2+1)\times d_y}$, where $d_y$ is the output dimension. The intermediate fusion tensor is calculated as follows:

$$Z_1 = X_1^{'} F_1 \in R^{B\times r\times d_y} \tag{3}$$

$$Z_2 = X_2^{'} F_2 \in R^{B\times r\times d_y} \tag{4}$$

where $Z_1$ and $Z_2 \in R^{B\times r\times d_y}$ are modality-specific intermediate representations. Then, cross-modal interaction characteristics are captured through element-wise multiplication:

$$Z_{12} = Z_1 \bigodot Z_2 \in R^{R\times r\times d_y} \tag{5}$$

where $Z_{12}$ is the joint tensor. The final output $Z \in R^{B\times r}$ is obtained by extracting the first dimension and transposing:

$$Z = Z_{12}[:,:,0]^T \in R^{B\times r} \tag{6}$$

Therefore, the output of Local Pairwise Fusion generates a compact feature vector of dimension r for each sample, where $r$ is the low-rank parameter reflecting the degree of compression of the fused representation. This representation not only efficiently preserves cross-modal correlations but also provides high-quality intermediate features for subsequent Global Triadic Fusion multimodal integration.

### 3.2.2 Global Triadic Fusion

Given three representations $H_1$,$H_2$,$H_3$ produced by the Modility-Specific Feature Extractor Encoder, The final output representation of the Global Triadic Fusion is $O \in R^{B\times d_y}$, with $d_y$ as the output dimension, which we set to the number of specific cancer subtype categories.

It is worth noting that the Global Triadic Fusion does not directly fuse the original hidden representations produced by the Modality-Specific Feature Extractor Encoder. Instead, it is built upon the results of three bimodal low-rank fusions described in Section.(3.2.1). This hierarchical design is first used to extract local interactions between modalities through pairwise fusion, and then applied to integrate global features via trimodal fusion. This enhances the model's robustness and expressive power in scenarios with modality imbalance.

The implementation of Global Triadic Fusion relies on a preceding pairwise fusion step. The specific process is as follows: Before Global Triadic Fusion, three Local Pairwise Fusions respectively fuse modality pairs to generate intermediate representations:

$$O_{12} = M_{12}(H_1, H_2) \tag{7}$$

$$O_{13} = M_{13}(H_1, H_3) \tag{8}$$

$$O_{23} = M_{23}(H_2, H_3) \tag{9}$$

Where $M_{ij}$ denotes the Local Pairwise Fusion, which outputs $O_{12}, O_{13}, O_{23} \in B^{B\times r}$, $r$ is the rank parameter, and each output is a compact feature vector of dimension $r$ corresponding to each sample.

Take the three pairs of fused intermediate representations $O_{12}, O_{13}, O_{23}$ as the input of the Global Triadic Fusion. Similarly, extend its hidden representation as:

$$\hat{O_{12}} = [1, O_{12}] \tag{10}$$

$$\hat{O_{13}} = [1, O_{13}] \tag{11}$$

$$\hat{O_{23}} = [1, O_{23}] \tag{12}$$

where $1 \in R^{B\times 1}$ is an all-one vector, and the extended representations are denoted as $\hat{O_{12}}, \hat{O_{12}}, \hat{O_{23}} \in R^{B\times(r+1)}$. Define low-rank factors for each intermediate representation as modality-specific factors $F_{12} \in R^{r^{'}\times(h_1+1)\times d_y}$, $F_{13} \in R^{r^{'}\times(h_2+1)\times d_y}$, $F_{23} \in R^{r^{'}\times(h_3+1)\times d_y}$, where $r^{'}$ is the rank parameter of the three-modality fusion, and $d_y$ is the final output dimension. Then, we use low-rank factors to transform the

expanded intermediate representation:

$$Z_{12} = \hat{O}_{12} F_{12} \tag{13}$$

$$Z_{13} = \hat{O}_{13} F_{13} \tag{14}$$

$$Z_{23} = \hat{O}_{23} F_{23} \tag{15}$$

where $Z_{12}, Z_{13}, Z_{23} \in R^{B \times r' \times d_y}$ represents pairs of intermediate tensors. Next, integrate the three intermediate tensors through element-wise multiplication:

$$Z_{123} = Z_{12} \bigodot Z_{13} \bigodot Z_{23} \tag{16}$$

Where $Z_{123} \in R^{B \times r' \times d_y}$ is the joint tensor that captures the global interaction information among all modalities. The joint tensor generates the final output through a weighted sum and bias calculation:

$$O = (W_f Z_{123}^T) + b_f \tag{17}$$

Where $W_f \in R^{1 \times r'}$ is the fusion weight matrix, $b_f \in R^{1 \times d_y}$ is the bias vector, and the reshaped output $O \in R^{B \times d_y}$ is the feature vector corresponding to each sample with dimension $d_y$.

Compared to Local Pairwise Fusion, Global Triadic Fusion performs hierarchical fusion, which not only preserves local interaction characteristics but also achieves efficient integration of global information.

### 3.3 Hierarchical Fusion Integrator

In the Triad-LMF framework, the fusion of multi-omics data is realized through a hierarchical structure to efficiently integrate heterogeneous information and generate a unified representation suitable for cancer subtype classification. The Hierarchical Fusion Integrator, a core component of this layered design, integrates Local Pairwise Fusion and Global Triadic Fusion step-by-step via the hierarchy, transitioning from local modality interactions to global information integration.

Given the imput multimodal omics data $X_1, X_2$ and $X_3$, its corresponding hidden representations are denoted as $H_1 \in R^{B \times h_1}$, $H_2 \in R^{B \times h_2}$ and $H_3 \in R^{B \times h_3}$, which are generated by the Modality-Specific Embedding Subnetwork. Here, $B$ represents the batch size, and $h_m$ denotes the hidden dimension of each modality. The Hierarchical Fusion Integrator employs a two-stage strategy:

- Two-Feature LMF module: Three Local Pairwise Fusion modules are applied to modality pairs, producing intermediate representations that capture local inter-modal interactions.
- Three-way LMF module: A Global Triadic Fusion module integrates the above intermediate representations to generate the final output, which can directly support cancer subtype classification tasks.

The Hierarchical Fusion Integrator optimizes the contributions of sparse modalities and balances the representation weights across modalities. Its performance will be validated in subsequent experiments.

# 4 EXPERIMENTS AND RESULTS

## 4.1 Dataset

We applied the proposed model to classification tasks on three different datasets. The first dataset is breast invasive carcinoma (BRCA), which includes CNV, mRNA, RPPA, and PAM50 subtype labels (including Her2, LumA, and LumB subtypes), sourced from the literature(Li et al. (2022)) . The second dataset is used for molecular subtype classification of STAD (including CIN, MSI, GS, and EBV subtypes), provided by the literature(Bu et al. (2024)). Both datasets contain a sufficient number of samples and a reasonable number of subtypes. Additionally, for BRCA cancer subtype classification, we introduced a third dataset: the PAM50 subtype classification of breast invasive carcinoma (BRCA_2) from TCGA. Compared to the BRCA dataset, which covers broader molecular levels, BRCA_2 focuses more on RNA regulatory mechanisms. All datasets are summarized in Table 1.

**Table 1.** Description of BRAC, STAD, BRAC_2 dataset

| **Dataset** | **Categories** | | | | **Number of Features** | | |
|---|---|---|---|---|---|---|---|
| BRAC | **Basal**<br>112 | **Her2**<br>53 | **LumA**<br>248 | **LumB**<br>98 | **RPPA**<br>223 | **CNV**<br>16383 | **RNA-seq**<br>16383 |
| STAD | **CIN**<br>173 | **MSI**<br>59 | **GS**<br>50 | **EBV**<br>19 | **methylation**<br>3287 | **miRNA**<br>702 | **mRNA**<br>4089 |
| BRAC_2 | **Basal**<br>118 | **Her2**<br>40 | **LumA**<br>356 | **LumB**<br>136 | **SNV**<br>6 | **miRNA**<br>6510 | **RNA-seq**<br>2616 |

It is worth noting that in the BRCA_2 dataset, the number of features in the SNV modality is only 6, showing a significant imbalance compared to miRNA (6510 features) and RNA-seq (2616 features). Such extreme differences in feature dimensions across modalities are common in multi-omics data. This significant imbalance among modalities may weaken the model's ability to capture sparse modalities when using traditional multimodal fusion methods (such as feature concatenation or tensor outer product), as high-dimensional ones can overshadow the contributions of low-dimensional modalities. The Triad-LMF model effectively addresses this challenge through its unique design, and its efficiency and robustness in imbalanced modality scenarios will be discussed in detail in Section 3. We preprocessed the data before applying the Triad-LMF model to ensure quality and consistency. First, patient samples with more than 10% missing information in any modality were excluded from the dataset. This threshold was chosen based on standard practices reported in the literature (Yin et al. (2022))while retaining sufficient samples to support statistical analysis. Second, features with more than 10% missing values across all patient samples were removed to avoid impairing the model's feature extraction capabilities due to incomplete information. These preprocessing steps transformed the multimodal data into a high-quality set, laying a solid foundation for modality-specific embedding and multimodal fusion.

## 4.2 Evaludation Metrics

To comprehensively quantify Triad-LMF's performance in cancer subtype multiclass classification tasks, we selected the following standard evaluation metrics.

$$Accuracy = \frac{TP + FP}{TP + TN + FP + FN}$$

$$Precision = \frac{TP}{TP + FP}$$

$$Recall = \frac{TP}{TP + FN}$$

$$F1 - score = 2 \times \frac{Precision \times Recall}{Precision + Recall}$$

Where $TP$ refers to samples that actually belong to a certain class and are correctly predicted as that class, while $TN$ refers to samples that the model correctly identifies as not belonging to the target class. For multi-class tasks, any class other than the positive class is defined as negative. $FP$ refers to samples the model incorrectly predicts as belonging to the target class, and $FN$ refers to samples that the model incorrectly predicts as not belonging to the target class. $Accuracy$, $Precision$, $Recall$, and $F1 - score$ are the most commonly used classification performance metrics based on the aforementioned $TP$, $TN$, $FP$, and $FN$. Considering the potential class imbalance in the dataset, we primarily report $F1 - score$ and $Accuracy$ to evaluate model performance comprehensively. To further ensure the reliability of the results, all performance comparisons are validated for significance using the Wilcoxon rank-sum test.

### 4.3 Experimental Setup

The implementation of Triad-LMF is based on the PyTorch framework, and training and testing were conducted on an NVIDIA GeForce RTX 3060 GPU. To ensure the model's stability and generalization capability, we performed a systematic hyperparameter optimization on the validation set through grid search, focusing on key parameters such as the learning rate, local fusion rank, global fusion rank, and dropout rate. Table 2 lists the candidate value ranges for the hyperparameters.

**Table 2.** Triad-LMF Hyperparameter Optimization Range

| Hyperparameter | Candidate value range |
|---|---|
| Learning Rate | $1e-3, 5e-4, 1e-4, 5e-5$ |
| Batch Size | 32, 64, 128 |
| Hidden Layer | 64, 128, 256 |
| $r$ | 2, 4, 8 |
| $r'$ | 4, 8, 16 |
| Weight Decay | $1e-4, 1e-5, 1e-6$ |
| Dropout | 0.1, 0.3, 0.5 |

Triad-LMF uses the cross-entropy loss function and minimizes the loss through the Adam optimizer. To prevent overfitting, we introduce an early stopping mechanism that terminates training when the validation loss does not decrease for 10 consecutive epochs. Additionally, it should be noted that Dropout is not mentioned in the table; we adjust the corresponding Dropout rates according to the characteristics of each modality to balance regularization effects. All experiments are repeated five times, reporting the metrics' mean and standard deviation to ensure the results' robustness and reproducibility. As shown in Table 3, the

final selected hyperparameter combination achieves excellent classification performance on the validation set.

**Table 3.** Key Experimental Setup Parameters

| Hyperparameter | Value | Hyperparameter | Value |
|---|---|---|---|
| Framework | PyTorch | Weight Decay | 1e-5 |
| Optimizer | Adam | $H_m$ | 128 |
| Learning Rate | 1e-4 | $r$ | 4 |
| Batch Size | 64 | $r'$ | 8 |
| Training Epochs | 100 | Early Stopping $\delta$ | 10 |
| Weight Decay | 1e-5 | Early Stopping Patience | 10 |
| Hardware Platform | NVIDIA GeForce RTX 3060 | | |

During training, we apply batch normalization to the preprocessed features $X_m$ to reduce input feature covariate shift. Moreover, we need to avoid overfitting in high-dimensional feature space since our datasets have a relatively small sample size. We applied Dropout regularization during training

### 4.4 Triad-LMF Outperforms Existing Comparative Cancer Subtype Diagnostic Methods in Standard Supervised Learning

To rigorously evaluate the performance of Triad-LMF, we compared it against a series of baseline methods and related advanced multi-omics fusion approaches on the BRCA and STAD datasets. The baseline methods were constructed as follows: 1.Naive multimodal fusion: directly concatenating feature vectors from all modalities, then inputting the concatenated high-dimensional features into traditional machine learning classifiers for training. 2.Advanced multi-omics fusion methods: Triad-LMF was further compared with MOGONET(Wang et al. (2021)). The same training-testing data splits were used across all comparative methods to ensure fairness in all experiments. Performance evaluation uniformly used the metrics defined in Section 3.1. The experimental results are shown in Table 4. On both the BRCA and STAD datasets, Triad-LMF consistently outperformed all baseline and comparative methods on key evaluation metrics. On the BRCA dataset, Triad-LMF achieved an F1 score of 0.8063, while the best-performing baseline method, RF, scored 0.8020. Similarly, as shown in Table 5 for the STAD dataset, Triad-LMF reached an Accuracy of 0.8947, surpassing the MODALIT method's 0.8197. These results demonstrate that our proposed hierarchical fusion strategy can effectively integrate information from different omics data types, thereby significantly improving the Accuracy of cancer subtype classification.

**Table 4.** Comparison of Triad-LMF Diagnostic Methods for Cancer Subtypes on BRCA Dataset

| Method | Accuracy | Precision | Recall | F1 |
|---|---|---|---|---|
| DT | $0.8350 \pm 0.021$ | $0.7500 \pm 0.030$ | $0.7730 \pm 0.028$ | $0.7537 \pm 0.027$ |
| KNN | $0.6117 \pm 0.035$ | $0.3960 \pm 0.045$ | $0.3382 \pm 0.040$ | $0.3155 \pm 0.042$ |
| GNB | $0.5728 \pm 0.038$ | $0.3233 \pm 0.048$ | $0.3441 \pm 0.045$ | $0.3265 \pm 0.046$ |
| RF | $0.8830 \pm 0.015$ | $0.8710 \pm 0.018$ | $0.8174 \pm 0.020$ | $0.8020 \pm 0.019$ |
| SVM | $0.8447 \pm 0.018$ | $0.8379 \pm 0.020$ | $0.7773 \pm 0.022$ | $0.7826 \pm 0.021$ |
| MOGONET | $0.8738 \pm 0.016$ | $0.8837 \pm 0.017$ | $0.7644 \pm 0.019$ | $0.7773 \pm 0.018$ |
| **Triad-LMF** | $\mathbf{0.8947 \pm 0.012}$ | $\mathbf{0.8950 \pm 0.013}$ | $\mathbf{0.8299 \pm 0.014}$ | $\mathbf{0.8063 \pm 0.013}$ |

**Table 5.** Comparison of Triad-LMF Diagnostic Methods for Cancer Subtypes on STAD Dataset

| Method | Accuracy | Precision | Recall | F1 |
|---|---|---|---|---|
| DT | $0.7377 \pm 0.025$ | $0.7480 \pm 0.030$ | $0.6614 \pm 0.032$ | $0.6880 \pm 0.030$ |
| KNN | $0.6885 \pm 0.028$ | $0.7456 \pm 0.035$ | $0.6038 \pm 0.038$ | $0.6278 \pm 0.036$ |
| GNB | $0.7049 \pm 0.027$ | $0.7438 \pm 0.034$ | $0.6057 \pm 0.037$ | $0.6368 \pm 0.035$ |
| RF | $0.8852 \pm 0.014$ | $0.8355 \pm 0.017$ | $0.8636 \pm 0.016$ | $0.8896 \pm 0.015$ |
| SVM | $0.8525 \pm 0.016$ | $0.8143 \pm 0.019$ | $0.8163 \pm 0.018$ | $0.8501 \pm 0.017$ |
| MOGONET | $0.8197 \pm 0.018$ | $0.8618 \pm 0.020$ | $0.7727 \pm 0.021$ | $0.7905 \pm 0.020$ |
| **Triad-LMF** | $\mathbf{0.8947 \pm 0.013}$ | $\mathbf{0.8445 \pm 0.015}$ | $\mathbf{0.8217 \pm 0.016}$ | $\mathbf{0.8997 \pm 0.014}$ |

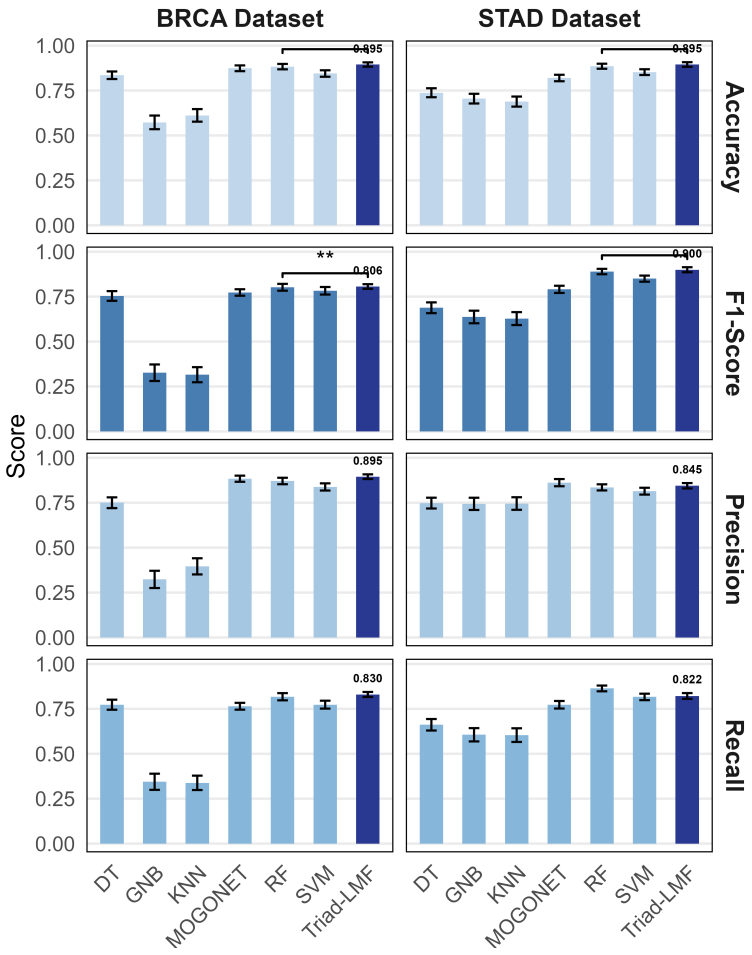


**Figure 2.** Triad-LMF outperforms existing cancer subtype diagnosis methods in standard supervised learning comparisons

## 4.5 Revealing the Latent Space Structure of Triad-LMF through UMAP

To qualitatively analyze the Triad-LMF model's ability to learn discriminative data representations during the hierarchical fusion process, we employed UMAP technology to reveal the model's progressive refinement of cancer subtype discriminatory information through two-dimensional visualization. UMAP is a nonlinear dimensionality reduction method that effectively preserves both local and global topological structures of high-dimensional data, making it suitable for evaluating the discriminability of latent space representations(McInnes et al. (2018)). Specifically, we extracted embedding vectors from four key stages of Triad-LMF's hierarchical fusion architecture: three Local Pairwise Fusion stages and one Global Triadic

Fusion stage. Based on test samples from the BRCA and STAD datasets, these vectors reflect the model's representational capability for cancer subtype classification at different fusion stages.

We applied UMAP to project the high-dimensional embedding vectors into a two-dimensional space to assess samples' clustering characteristics and inter-cluster separability in the latent space. As shown in Figure 3, during the Local Pairwise Fusion stages, the model already demonstrated preliminary subtype differentiation ability, with samples of the same subtype forming loose clusters and cluster boundaries exhibiting some level of separability. However, the final latent space representation after Global Triadic Fusion significantly outperformed the earlier stages, evidenced by tighter subtype clusters and more precise boundaries between clusters. These visualizations reveal the mechanism by which Triad-LMF progressively enhances representational discriminability through modal synergy, validating the effectiveness of its hierarchical fusion architecture in integrating multi-modal information.

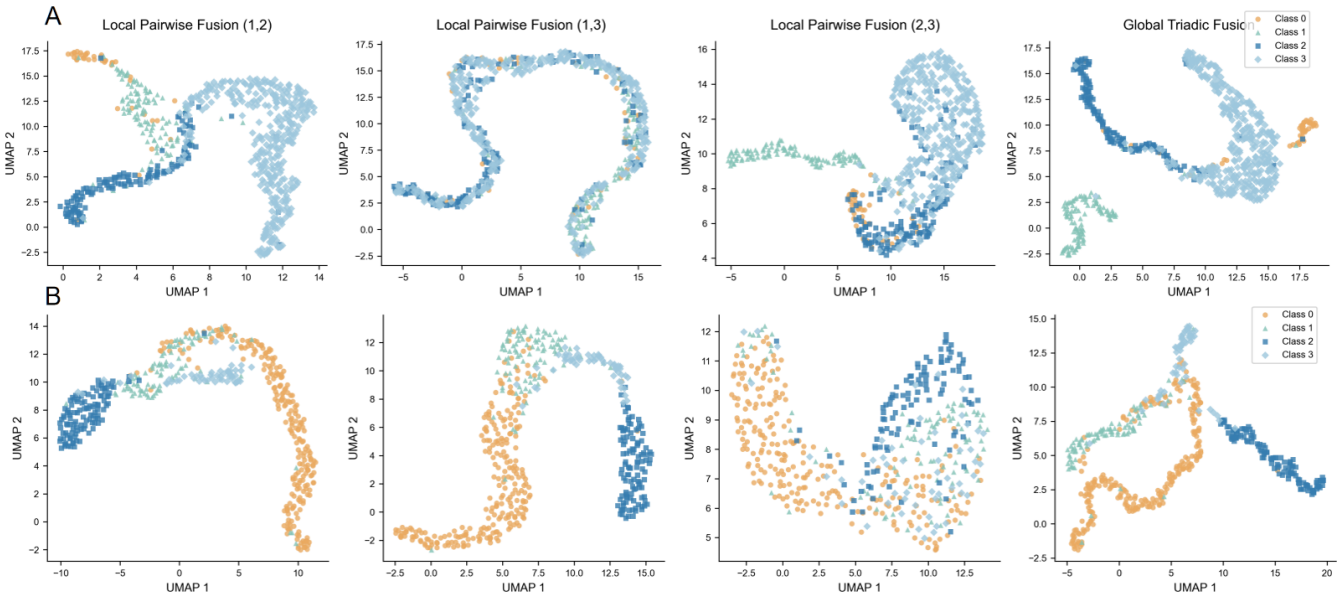


**Figure 3.** UMAP Visualization of STAD (A) and BRCA (B)

## 4.6 Ablation study

To quantitatively evaluate the contributions of each key component in the Triad-LMF framework—notably the Local Pairwise Fusion and Global Triadic Fusion—to the overall model performance, we designed and conducted a series of ablation experiments using the BRCA dataset. These experiments investigated the impact on performance metrics by sequentially removing certain components of Triad-LMF or replacing specific parts of the framework. The training loss dynamics are shown in Figure 4(A), and the final classification performance comparison is presented in Figure 4(B). The proposed Triad-LMF framework achieves the best performance in terms of the ACC metric, confirming its overall effectiveness. In contrast, removing any Local Pairwise Fusion module from Triad-LMF causes a significant drop in Accuracy, indicating that pairwise cross-modal interactions are crucial for enhancing classification performance and that the model effectively extracts valuable discriminative features from the fusion of modal pairs. Notably, when the Global Triadic Fusion is removed and replaced with simple concatenation, the model's performance falls short of the full Triad-LMF and underperforms compared to the baseline model. This

result highlights that simply obtaining pairwise fused features is insufficient; the subsequently designed low-rank tri-modal fusion mechanism is essential for effectively integrating information from all three pairwise interactions and capturing higher-order complex relationships rather than merely summing the information. Through systematic ablation experiments, we confirm that each core component of the Triad-LMF model contributes positively to the final performance. Removing any single component leads to a performance decline. This fully validates the rationality and effectiveness of our proposed hierarchical, two-stage fusion architecture, demonstrating that Triad-LMF can fully leverage both pairwise cross-modal interactions and higher-order tri-modal integrated information to achieve superior cancer subtype classification performance.

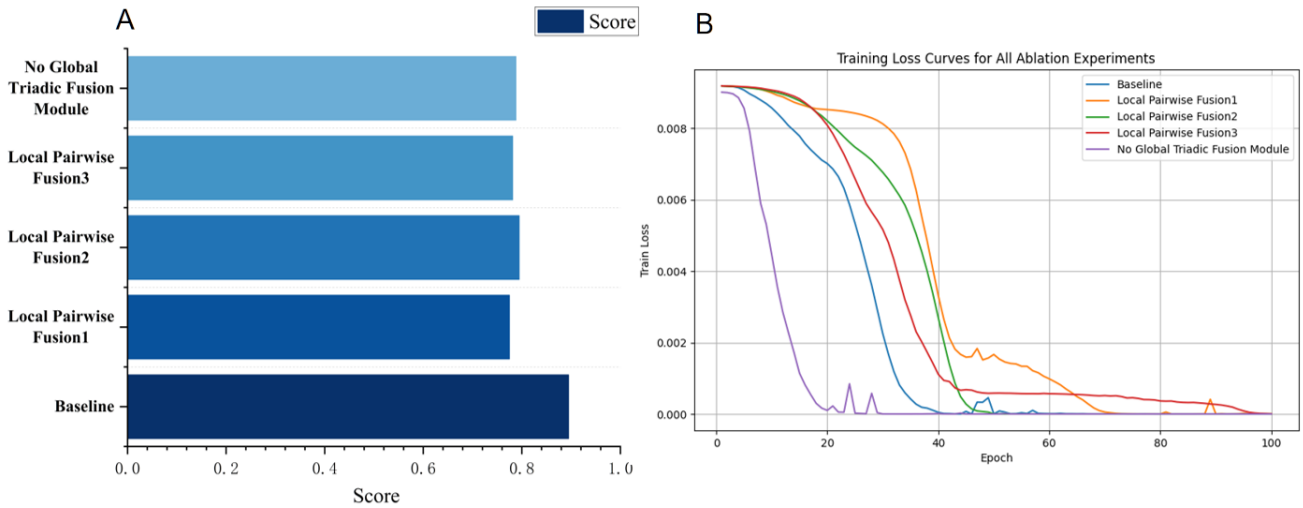


**Figure 4.** (A) BRCA ablation experiment Accuracy bar chart (B) BRCA ablation experiment loss function line chart (Local Pairwise Fusion1: removed the fusion of modalities 1 and 2 from the baseline. Local Pairwise Fusion2: removed the fusion of modalities 2 and 3 from the baseline. Local Pairwise Fusion3: removed the fusion of modalities 2 and 3 from the baseline. No Global Triadic Fusion: removed Global Triadic Fusion from the baseline, replaced with simple concatenation.)

## 4.7 Feature Importance Analysis and Biological Interpretation based on SHAP

To explain the cancer subtype classification mechanism of Triad-LMF and explore its biological significance, we employed the SHapley Additive exPlanations (SHAP) method(Lundberg and Lee (2017))for a systematic analysis of feature importance in Triad-LMF. SHAP is a model interpretability tool based on game theory that quantifies the marginal contribution of each input feature to the model output, providing both global and local assessments of feature importance. We calculated SHAP values for all features in the test set of the BRCA dataset, with a focus on the features with the highest overall contributions and those that have a significant impact on the classification of specific cancer subtypes. Using SHAP's TreeExplainer, we analyzed the prediction results of the Triad-LMF model, computed SHAP values for each feature, and ranked the features based on their mean absolute SHAP values. Table 6 lists the top 60 ranked features, encompassing key proteins, phosphorylation sites, and other biomarkers. These features play important roles in the molecular mechanisms of breast cancer, reflecting the model's sensitivity to biologically relevant signals. Additionally, as shown in Figure 5(C), we present the sensitivity of the four BRCA subtype categories to the significant features.

As shown in Table 6, the top-ranked features show the precision of the Triad-LMF model in capturing the key nodes of breast cancer biology. Ribosomal protein S6 is a core downstream effector of the mTOR

**Table 6.** Top 60 Features Identified by Triad-LMF on the BRCA Dataset Based on SHAP

| Rank | Feature | Rank | Feature | Rank | Feature |
|---|---|---|---|---|---|
| 1 | S6 | 21 | EGFR_pY1173 | 41 | PDK1 |
| 2 | ERALPHA | 22 | S6_pS235S236 | 42 | PTEN |
| 3 | PR | 23 | SRC_pY527 | 43 | CYCLINE1 |
| 4 | P27_pT198 | 24 | G6PD7 | 44 | MYH11 |
| 5 | BCL2 | 25 | CYCLINB1 | 45 | GATA3 |
| 6 | P90RSK_pT359S363 | 26 | DVL3 | 46 | TFRC |
| 7 | CAVEOLIN1 | 27 | TUBERIN_pT1462 | 47 | PI3KP110ALPHA |
| 8 | EEF2 | 28 | ERALPHA_pS118 | 48 | ANNEXIN1 |
| 9 | EGFR | 29 | JAK2 | 49 | MAPK_pT202Y204 |
| 10 | IRS1 | 30 | LCK | 50 | BIM |
| 11 | SYK | 31 | AMPKALPHA_pT172 | 51 | CASPASE3 |
| 12 | CASPASE7CLEAVEDD198 | 32 | ANNEXINVII | 52 | SCD1 |
| 13 | PAXILLIN | 33 | EGFR_pY1068 | 53 | AMPKALPHA |
| 14 | HER3 | 34 | XRCC1 | 54 | RICTOR |
| 15 | ASNS | 35 | RBM15 | 55 | MYOSINIIA_pS1943 |
| 16 | RICTOR_pT1135 | 36 | IGFBP2 | 56 | GATA6 |
| 17 | MYOSINIIA | 37 | AR | 57 | HER2 |
| 18 | ACETYLATUBULINLYS40 | 38 | PARPCLEAVED | 58 | RAB11 |
| 19 | HER2_pY1248 | 39 | PDL1 | 59 | PCADHERIN |
| 20 | GSK3ALPHABETA | 40 | STAT3_pY705 | 60 | CHK2 |

signaling pathway, regulating protein synthesis and cell proliferation. Its significant ranking suggests that Triad-LMF is highly sensitive to mTOR-driven tumor proliferation. Aberrant activation of the mTOR signaling pathway is widespread in breast cancer and is closely associated with tumor progression and treatment resistance(Choi et al. (2010)). The primacy of S6 in the SHAP analysis is consistent with the clinical efficacy of mTOR inhibitors (e.g., everolimus), which studies have shown to significantly improve the prognosis of patients with hormone receptor-positive breast cancer (Engelman (2009);Yardley et al. (2013)).ERALPHA and PR are signature molecules of the LumA and LumB subtypes that regulate hormone-dependent gene expression and tumor cell proliferation. The high ranking reflects the model's prioritized focus on hormonal signaling pathways, which is highly consistent with breast cancer molecular typing studies (Perou et al. (2000)).ERALPHA expression level is a key predictor of the efficacy of endocrine therapies (e.g., tamoxifen), and PR expression further refines prognostic assessment of the Luminal subtype(Osborne and Schiff (2011);Horwitz et al. (2008)). The ability of Triad-LMF to recognize both underscores its Precision in the classification of hormone receptor-positive breast cancer.P27_pT198 and BCL2 are involved in cell cycle regulation and anti-apoptotic mechanisms, respectively.P27, through the phosphorylation site T198 regulates nucleoplasmic localization and cell cycle progression, and its high ranking suggests that the model focuses on cell cycle dysregulation in breast cancer progression(Sherr and Roberts (1999)). It has been shown that P27 phosphorylation correlates with poor prognosis, reflecting the active state of tumor proliferation (Viglietto et al. (2002)).BCL2, as an anti-apoptotic protein, inhibits programmed cell death and promotes tumor survival. It is often highly expressed, especially in Luminal subtypes. The prominent ranking of BCL2 in the SHAP analysis suggests that the model effectively captures the tumor survival mechanisms, consistent with its role in breast cancer prognosis and treatment response (Dawson et al. (2010);Callagy et al. (2006)). eGFR_pY1068, HER2_pY1248, and MAPK_pT202Y204 mark the activation status of EGFR, HER2, and MAPK/ERK signaling pathways, respectively. These features

are particularly prominent in HER2+ subtypes, driving cell proliferation and survival.HER2_pY1248 is a key target for targeted therapies (e.g., trastuzumab), whereas MAPK_pT202Y204 is associated with tumor invasion and metastasis (Hynes and Lane (2005)). The high ranking of EGFR_pY1068 is further suggestive of the model's identification of the EGFR signaling pathway in breast cancer heterogeneity (Roberts and Der (2007)). The outstanding contribution of these features suggests that the model Triad-LMF accurately captures the dynamics of the signaling network, consistent with the complexity of breast cancer molecular mechanisms (Lord and Ashworth (2016)). In addition, PI3KP110ALPHA, PTEN, GATA3, and PDL1 regulate the PI3K/AKT pathway, differentiation characteristics of Luminal subtypes, and immune escape mechanisms in TNBC, respectively.PI3KP110ALPHA and PTEN co-regulate the PI3K signaling pathway, which is closely associated with tumor proliferation and treatment resistance (Thorpe et al. (2015);Lee and Song (2012)).GATA3, as a transcription factor, is associated with the hyper differentiation characteristics of the Lum subtype, and its ranking reflects the model's focus on subtype-specific features (Ellis et al. (2012)).PDL1, on the other hand, is a key molecule for immune escape in TNBC, which is correlated with the efficacy of immune checkpoint inhibitors, suggesting that the model integrates the tumor microcircuits with the tumor microcircuits—correlates, suggesting that the model integrates tumor microenvironmental features (Mittendorf et al. (2019)). Identifying these features further validates the model's ability to integrate signal transduction, molecular differentiation, and immune regulation.

The top 60 features identified by SHAP are highly consistent with the known molecular mechanisms of breast cancer, encompassing mTOR, hormone receptors, PI3K/AKT, EGFR/HER2, and immune-related pathways. This validates the Triad-LMF model's biological interpretability and highlights its potential application value in Precision medicine, providing an important basis for biomarker validation and targeted therapy research. Next, we conducted a Gene Ontology (GO)(**?**)on the top 60 high-ranking features, focusing on the Biological Process category. The results showed significant enrichment ($p < 0.05$) in key pathways, including (1) negative regulation of programmed cell death involving BCL2, CASPASE7CLEAVEDD198, CASPASE3, and BIM, underscoring tumor anti-apoptotic mechanisms closely related to breast cancer cell survival and therapy resistance(Dawson et al. (2010);Czabotar et al. (2014)); (2) regulation of DNA recombination, including XRCC1 and CHK2, reflecting the role of DNA repair and genome stability in BRCA1/2 mutant subtypes(Roy et al. (2011);O'Donovan and Livingston (2010)); (3) phosphatidylinositol-mediated signaling, covering IRS1, PDK1, and PI3KP110ALPHA, pointing to the PI3K/AKT/mTOR pathway, which is associated with tumor proliferation and resistance to targeted therapies(Thorpe et al. (2015);Engelman (2009)). These pathways are highly consistent with the molecular mechanisms of breast cancer, for example, the PI3K/AKT pathway driving cell survival(Fruman and Rommel (2017)) and DNA repair influencing genome instability subtypes (Lord and Ashworth (2016)). Figure 5(B) visually illustrates the associations between these pathways and genes, while Figure 5(C) further quantifies pathway significance and gene counts. We confirmed that the Triad-LMF model can achieve interpretable subtype classification by capturing key biological processes.

## 4.8 Validating Effectiveness using other BRCA datasets

To evaluate the robustness and generalization ability of the Triad-LMF framework, we applied it to the BRCA_2 dataset. This dataset features the same cancer types and subtypes as BRCA but utilizes a different combination of omics modalities. We trained and evaluated the Triad-LMF model on the BRCA_2 dataset using the same hyperparameter settings applied to the original BRCA dataset.

Triad-LMF also demonstrated strong performance on the BRCA_2 dataset, achieving an Accuracy of 0.9237, as shown in Figure 6. Although the direct comparison of absolute performance scores between

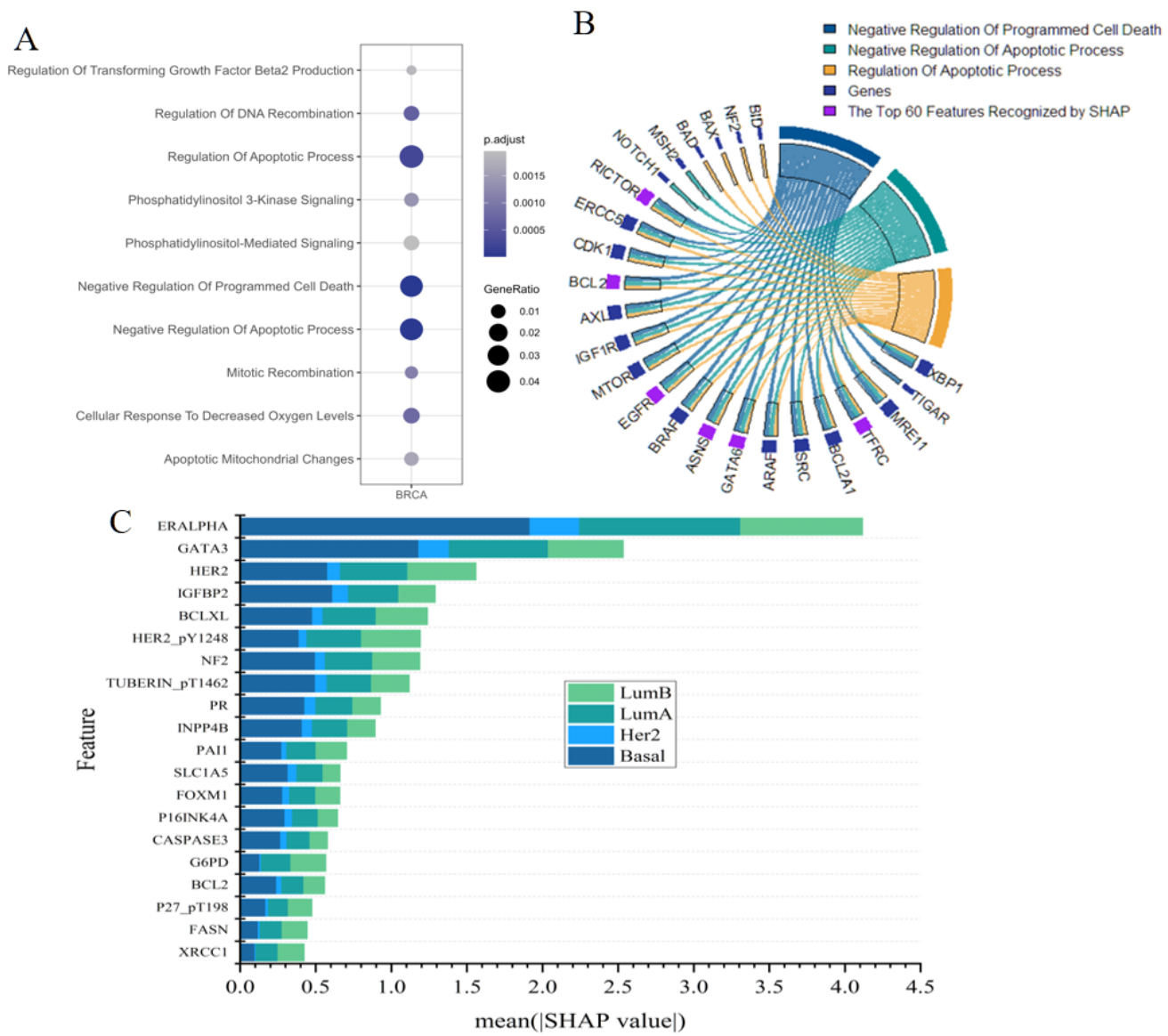


**Figure 5.** (A) GO functional enrichment analysis results of the top 60 features. (B) Average absolute SHAP values of the top 60 features. (C) Sensitivity of four BRCA dataset categories to significant features.

BRCA and BRCA_2 is complicated due to differences in data modalities and underlying patient cohorts, the high performance achieved on BRCA_2 indicates that the proposed Triad-LMF framework is not limited to specific combinations of omics data types. It successfully adapts to different modalities while maintaining its effectiveness in classifying the same biological subtypes. This supports the universality and robustness of the hierarchical fusion strategy we proposed for multi-omics cancer data integration.

## 5 DISCUSSION

In cancer research, multi-omics data integration plays a crucial role in revealing the complexity of diseases and improving diagnostic Accuracy. Our proposed Triad-LMF model features a hierarchical fusion architecture that integrates progressively from local modality interactions to global information consolidation through the Two-Feature LMF module and Three-way LMF modules. This effectively captures the complex interactions among multi-omics data, demonstrating promising application potential.

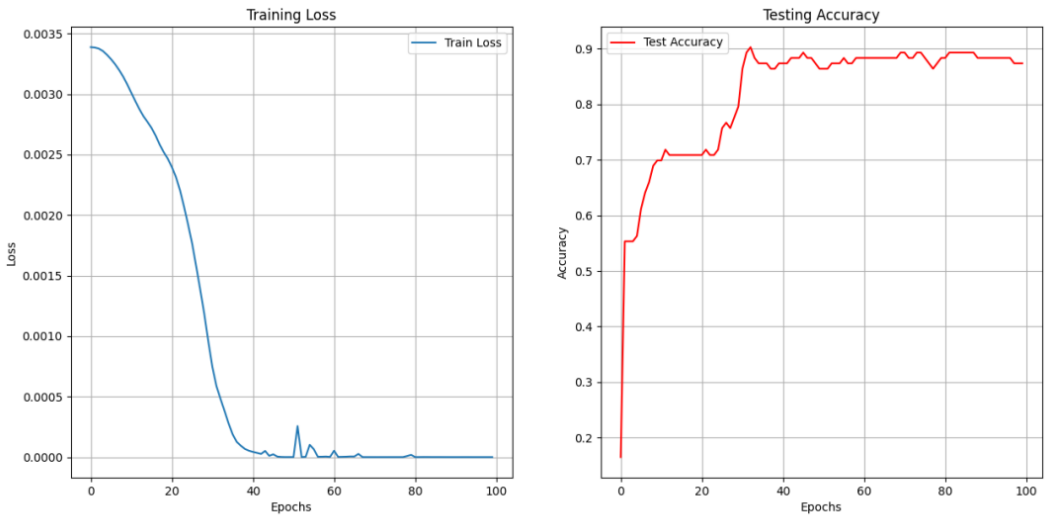


**Figure 6.** Performance of Triad-LMF on the BRCA_2 Dataset.

However, although the Triad-LMF model performs well overall, it was found in pairwise subtype classification results that tri-modal fusion may introduce noise in specific tasks, leading to performance that is inferior to single-modal or dual-modal combinations. This indicates that balancing information integration and noise control during the fusion process is a key challenge. In the future, we plan to explore more adaptive fusion mechanisms by dynamically optimizing modality selection and fusion weights to mitigate the impact of redundant information, thereby enhancing model robustness and Accuracy. Additionally, given the complexity and diversity of cancer research, we intend to expand the model to incorporate more types of omics data. Considering the efficiency and generalizability of Triad-LMF, we believe that through these improvements and extensions, the model will play a more critical role in pan-cancer subtype classification, biomarker discovery, and precision medicine research, providing a more powerful tool to advance multi-omics-driven cancer studies and accelerate the individualization and precision of cancer diagnosis and treatment. Moreover, in the absence of considering label noises, which some subtypes might be mislabeled (Chen et al. (2025)), future work could focus on developing robust methods against label noises.

## 6 CONCLUSION

This study proposes a deep learning framework called Triad-LMF based on low-rank multimodal fusion, aiming to address the challenges of integrating multi-omics data for cancer subtype classification. Through extensive experiments on BRCA, STAD, and BRCA_2 datasets, we demonstrate the significant advantages of Triad-LMF in classification performance, robustness, and generalization ability. Experimental results show that Triad-LMF achieved an F1 score of 0.8063 on the BRCA dataset, 0.8997 on the STAD dataset, and an Accuracy of 0.9237 on the BRCA_2 dataset, surpassing traditional machine learning baselines and advanced multi-omics fusion methods such as MOGONET. UMAP visualization validated the critical role of Global Triadic Fusion in enhancing the latent space's ability to distinguish subtypes, manifested by more compact subtype clusters and clearer boundaries between clusters. Ablation studies further confirmed the necessity of both Local Pairwise Fusion and Global Triadic Fusion; removing either component led to performance degradation, highlighting the synergistic effect of the hierarchical fusion architecture. SHAP-based feature importance analysis

These findings provide important evidence for identifying subtype-specific biomarkers and developing targeted therapeutic strategies.

## CONFLICT OF INTEREST STATEMENT

The authors declare that the research was conducted in the absence of any commercial or financial relationships that could be construed as a potential conflict of interest.

## AUTHOR CONTRIBUTIONS

XC conceptualized the project, XT and XC wrote and edited the original manuscript. XT and XC performed coding. XT conducted experiments. RT and ZR visualized the results. MJ curated the data. DY and XG edited the manuscript. All authors read and approved the final manuscript.

## FUNDING

This work was supported by the National Natural Science Foundation of China (12271068)

## ACKNOWLEDGMENTS

The authors would like to thank Professor Yuanshun Tan and Associate Professor Yu Mou for their valuable guidance on the manuscript, and would also like to thank Xiaofeng Chen for assistance with the experiments and Associate Mr. Xiongtao Xiao for valuable discussion.

## DATA AVAILABILITY STATEMENT

The original contributions presented are available upon further inquiries and can be directed to the corresponding authors.

## REFERENCES

Bu, Y., Liang, J., Li, Z., Wang, J., Wang, J., and Yu, G. (2024). Cancer molecular subtyping using limited multi-omics data with missingness. *PLOS Computational Biology* 20, e1012710. doi:10.1371/journal.pcbi.1012710

Callagy, G. M. et al. (2006). Bcl2 is a prognostic marker in breast cancer. *Journal of Clinical Pathology* 59, 478

Chen, X., Lin, S., Chen, X., Li, W., and Li, Y. (2025). Timestamp calibration for time-series single cell rna-seq expression data. *Journal of Molecular Biology* 437, 169021

Chen, X., Wang, Y., Zhang, Z., Zhang, J., and Zhang, Y. (2020). Deep-learning approach to identifying cancer subtypes using high-dimensional omics data. *Bioinformatics* 36, 1476–1483. doi:10.1093/bioinformatics/btz769

Choi, J. et al. (2010). mtor signaling and its involvement in cancer. *Cancer Research* 70, 9751

Czabotar, P. E. et al. (2014). Control of apoptosis by the bcl-2 protein family: Implications for physiology and therapy. *Nature Reviews Molecular Cell Biology* 15, 49–63. doi:10.1038/nrm3722

Dawson, S. J. et al. (2010). Bcl2 in breast cancer: A review and meta-analysis. *Modern Pathology* 23, 634–642

Ellis, M. J. et al. (2012). Whole-genome analysis informs breast cancer response to aromatase inhibition. *Nature*

Engelman, J. A. (2009). Targeting the pi3k/akt/mtor pathway in cancer. *Nature Reviews Cancer* 9, 550–562. doi:10.1038/nrc2656

Fruman, D. A. and Rommel, C. (2017). The pi3k pathway in human disease. *Cell* 170, 605–635. doi:10.1016/j.cell.2017.07.029

Gao, X. et al. (2022). Investigating semi-supervised learning for cancer subtype classification using small sample data. *IEEE Access* 10, 10912–10924. doi:10.1109/ACCESS.2022.3147261

Guo, Y. et al. (2020). Kernel fusion method for detecting cancer subtypes via selecting relevant expression data. *Frontiers in Genetics* 11, 979. doi:10.3389/fgene.2020.00979

Horwitz, K. B. et al. (2008). Progesterone receptor action: Defining a role in breast cancer. *Breast Cancer Research*

Hynes, N. E. and Lane, H. A. (2005). Erbb receptors and cancer: the complexity of targeted inhibitors. *Nature Reviews Cancer* 5, 341–354. doi:10.1038/nrc1609

Kuang, L., Zhang, Y., Li, X., Zhang, J., and Zhang, Z. (2023). Sadln: A deep learning model for cancer subtype classification using sparse autoencoder and deep neural network. *Bioinformatics* 39, btad353. doi:10.1093/bioinformatics/btad353

Lee, C.-H. and Song, J. (2012). Functions of parental involvement and effects of school climate on bullying behaviors among south korean middle school students. *Journal of School Violence* 11, 247–262. doi:10.1080/15388220.2012.682268

Li, X., Wang, Y., Zhang, Q., et al. (2024). Deepmoic: Multi-omics data integration via deep graph convolutional networks for cancer subtype classification. *BMC Genomics* 25, 1–15. doi:10.1186/s12864-024-11112-5

Li, X. et al. (2022). Mogcn: A multi-omics integration method based on graph convolutional network for cancer subtype analysis. *Frontiers in Genetics* 13, 806842. doi:10.3389/fgene.2022.806842

Lin, Y., Zhang, W., Cao, H., Li, G., and Du, W. (2020). Classifying breast cancer subtypes using deep neural networks based on multi-omics data. *Genes* 11, 888. doi:10.3390/genes11080888

Liu, X. et al. (2021). Multi-view spectral clustering based on multi-smooth representation fusion (mrf-msc). *Frontiers in Genetics* 12, 718915. doi:10.3389/fgene.2021.718915

Liu, Y. et al. (2024). Multifusion: A self-supervised multi-fusion strategy network for cancer subtype discovery. *Frontiers in Genetics* 15, 39610828. doi:10.3389/fgene.2024.39610828

Lord, C. J. and Ashworth, A. (2016). Brcaness revisited. *Nature Reviews Cancer* doi:10.1038/nrc.2015.21

Lundberg, S. M. and Lee, S.-I. (2017). A unified approach to interpreting model predictions. *Advances in Neural Information Processing Systems* 30

McInnes, L., Healy, J., Saul, N., and Großberger, L. (2018). Umap: Uniform manifold approximation and projection. *Journal of Open Source Software* 3, 861. doi:10.21105/joss.00861

Mittendorf, E. A. et al. (2019). Pd-l1 expression in triple-negative breast cancer. *Nature Reviews Clinical Oncology* doi:10.1038/s41571-019-0218-0

O'Donovan, M. and Livingston, D. M. (2010). Brca1 and brca2: breast/ovarian cancer susceptibility gene mutations and their clinical implications. *British Journal of Cancer* 103, 937–943. doi:10.1038/sj.bjc.6605881

Osborne, C. K. and Schiff, R. (2011). Mechanisms of endocrine resistance in breast cancer. *Annual Review of Medicine* doi:10.1146/annurev-med-070909-182917

Perou, C. M. et al. (2000). Molecular portraits of human breast tumours. *Nature* 406, 747–752. doi:10.1038/35021093

Ramirez, J., Smith, A., Zhang, Q., et al. (2022). Moanna: Multi-omics autoencoder-based neural network algorithm for predicting breast cancer subtypes. *ResearchGate*

Roberts, P. J. and Der, C. J. (2007). Targeting the raf-mek-erk mitogen-activated protein kinase cascade for the treatment of cancer. *Oncogene* 26, 3291–3310. doi:10.1038/sj.onc.1210422

Roy, R., Chun, J.-J., and Powell, S. N. (2011). Brca1 and brca2: different roles in a common pathway of genome protection. *Nature Reviews Cancer* 11, 104–112. doi:10.1038/nrc2985

Sahay, S., Okur, E., Kumar, S. H., and Nachman, L. (2020). Low rank fusion based transformers for multimodal sequences. In *Proceedings of the Second Grand-Challenge and Workshop on Multimodal Language (Challenge-HML)* (Association for Computational Linguistics), 29–34. doi:10.18653/v1/2020.challengehml-1.4

Sherr, C. J. and Roberts, J. M. (1999). Cdk inhibitors: positive and negative regulators of g1-phase progression. *Genes & Development* 13, 1501–1512. doi:10.1101/gad.13.12.1501

Singh, R. et al. (2022). Deepcsd: A minimalist deep learning framework for colorectal cancer subtype identification. *BMC Bioinformatics* 23. doi:10.1186/s13040-022-00301-2

Sun, L. et al. (2022). Coexpression module-based multi-class classification for cancer subtyping. *Frontiers in Genetics* 13, 866005. doi:10.3389/fgene.2022.866005

Thorpe, L. M. et al. (2015). Pi3k in cancer: Divergent roles of isoforms, modes of activation and therapeutic targeting. *Nature Reviews Cancer* 15, 7–24. doi:10.1038/nrc3860

Viglietto, G. et al. (2002). Cytoplasmic relocalization and inhibition of the cyclin-dependent kinase inhibitor p27(kip1) by pkb/akt-mediated phosphorylation in breast cancer. *Nature Medicine* 8, 1136–1144. doi:10.1038/nm762

Wang, Y., Zhang, Q., Li, X., et al. (2023). Autoggn: Autoencoder-based graph neural network for cancer multi-omics data integration. *Journal of Computational Biology* 30, 987–1001. doi:10.1089/cmb.2023.0123

Wang, Y., Zhang, Q., Li, X., et al. (2024). Mvgnn: Multi-view graph neural network for integrating multi-omics data in cancer subtype classification. *IEEE Transactions on Neural Networks and Learning Systems* 35, 1234–1245. doi:10.1109/TNNLS.2024.1234567

Wang, Y. et al. (2021). Mogonet: Integrating multi-omics data using graph convolutional networks for cancer subtype classification. *Nature Communications* 12. doi:10.1038/s41467-021-24574-9

Wu, X. et al. (2022). Deepgraphmut: Deep learning for cancer subtype classification using mutation data. *IEEE Access* 10, 10912–10924. doi:10.1109/ACCESS.2022.3183712

Yang, H., Li, J., Wang, Y., Zhang, Z., and Zhang, J. (2019). Bcdforest: a boosting cascade deep forest model towards the classification of cancer subtypes based on gene expression data. *Bioinformatics* 35, 2056–2063. doi:10.1093/bioinformatics/btz769

Yardley, D. A. et al. (2013). Everolimus plus exemestane in postmenopausal patients with hr+ breast cancer: Bolero-2 final progression-free survival analysis. *Journal of Clinical Oncology* doi:10.1200/JCO.2012.48.7908

Yin, C., Cao, Y., Sun, P., Zhang, H., Li, Z., Xu, Y., et al. (2022). Molecular subtyping of cancer based on robust graph neural network and multi-omics data integration. *Frontiers in Genetics* 13, 884028. doi:10.3389/fgene.2022.884028

Zhang, J. et al. (2022). Cancer molecular subtyping using limited multi-omics data. *PLOS Computational Biology* 18, e1012710. doi:10.1371/journal.pcbi.1012710

Zhao, Y. et al. (2022). Semihisnet: Semi-supervised learning for cancer subtype classification using consistency regularization. *Frontiers in Oncology* 12. doi:10.3389/fonc.2022.847324